DTU Library

Thermal profile detection through high-sensitivity fiber optic chirped Bragg grating on microstructured PMMA fiber

Korganbayev, Sanzhar; Rui, Min; Jelbuldina, Madina; Hu, Xuehao; Caucheteur, Christophe; Bang, Ole; Ortega, Beatriz; Marques, Carlos; Tosi, Daniele

Link back to DTU Orbit

Thermal profile detection through high-sensitivity fiber optic chirped Bragg grating on microstructured PMMA fiber

Sanzhar Korganbayev, Rui Min, Madina Jelbuldina, Xuehao Hu, Christophe Caucheteur, Ole Bang, Beatriz Ortega, Carlos Marques, Daniele Tosi

Abstract—In this work, a linearly chirped fiber Bragg grating (CFBG) inscribed in a microstructured polymer optical fiber (mPOF) has been demonstrated for detecting temperature profiles during thermal treatments. A CFBG of 10 mm length and 0.98 nm bandwidth has been inscribed in a mPOF fiber by means of a KrF laser and uniform phase mask. The CFBG has a high temperature sensitivity of -191.4 pm/$^\circ$C. The CFBG has been used as a semi-distributed temperature sensor, capable of detecting the temperature profile along the grating length, for scenarios that account minimally invasive biomedical treatments. Two experiments have been designed to validate the CFBG temperature reconstruction, using a linear gradient, and a research-grade radiofrequency ablation (RFA) setup to apply Gaussian-shaped temperature spatial profiles. The result is that the higher sensitivity of the CFBG supports the detection of spatially non-uniform temperature fields by means of spectral reconstruction.

Index Terms—optical fiber sensors; fiber Bragg grating (FBG); chirped FBG (CFBG); distributed temperature sensor (DTS); polymer optical fiber sensors; thermal ablation.

I. INTRODUCTION

ESTABLISHED over two decades, optical fiber sensors for measurement of temperature have been demonstrated and implemented in several applications in harsh environments, oil and gas, and industrial monitoring [1]. Fiber Bragg Grating (FBG) sensors [2],[3],[4] are the most popular technology for

S. Korganbayev, M. Jelbuldina, and D. Tosi are with Nazarbayev University, School of Engineering, 010000 Astana, Kazakhstan. D. Tosi is also with Laboratory of Biosensors and Bioinstruments, National Laboratory Astana (e-mail: skorganbayev@nu.edu.kz, madina.jelbuldina@nu.edu.kz, daniele.tosi@nu.edu.kz).

R. Min and B. Ortega are with ITEAM Research Institute, Universitat Politècnica de València, Valencia, Spain (e-mail: rumi@doctor.upv.es, bortega@dcom.upv.es).

X. Hu and C. Caucheteur are with Electromagnetism and Telecommunication Department, Université de Mons, 31 Boulevard Dolez, Mons, 7000, Belgium (e-mail: xuehao.hu@umons.ac.be, christophe.caucheteur@umons.ac.be).

O. Bang is with DTU Fotonik, Department of Photonics Engineering, Technical University of Denmark, Denmark (e-mail: oban@fotonik.dtu.dk).

C. Marques is with Instituto de Telecomunicações, Campus of Santiago, 3810-193 Aveiro, Portugal (e-mail: carlos.marques@ua.pt).

multi-point measurement, and present systems enable sensing networks with up to hundreds of sensing points with spatial resolution at the centimeter scale [5]. On the other side, distributed temperature sensors based on Raman scattering enable long-haul distributed sensing, for distances up to tens of kilometers and spatial resolution 10-100 cm [6].

One of the most recent challenges for fiber optic temperature sensing technologies is the application in healthcare [7]. In this framework, FBG sensors represent an effective technology, thanks to their miniature size and compact form factor, electromagnetic compatibility, biocompatibility in compliance to ISO 10993 standard, and possibility to be embedded in commercial catheters. However, an essential feature of fiber optic sensors for medical applications is the possibility to detect temperature spatial distributions, often labeled thermal maps [8] (temperature as a function of space and time), with a narrow spatial resolution and on the same fiber. The spatial resolution is defined as the distance between each sensing point. FBG sensors have small length (1-5 mm typically) and can operate in wavelength-division multiplexing [9]; with present draw-tower inscription setups they can achieve a centimeter-level spatial resolution for medical applications [10], while maintaining the fiber protective jacket. An alternative to FBG sensors is represented by optical frequency-domain backscatter reflectometry (OFDR) [11],[12], which is based on a white-light interferometer that detects the small Rayleigh backscatter signature of the fiber. OFDR system can further reduce the spatial resolution below the millimeter while maintaining a measurement time close to 1 Hz. However, distributed sensing system based on OFDR [13],[14] are built on interferometers with a reference trigger, that constitute a bulky optical hardware, that requires a swept-laser interferometer [13] or a microwave photonic circuit [14]. In addition, distributed systems do not have a specific active (or sensing) region in which the change of reflectivity is detected and encoded into a change of spectrum, but rather the entire fiber acts as a sensor along its entire length.

The possibility of measuring temperature pattern within a 15-50 mm with a sub-centimeter spatial resolution, region through a compact biocompatible sensor has a significant impact in medical devices. A major field of application is in the monitoring of minimally invasive thermo-therapies for cancer care [15], whereas a miniature applicator for microwave [16], radiofrequency (RF) [17], or laser [18] delivers a highly spatially confined heat field. In this application,

thermal gradients have slopes reaching 3-5°C/mm and 1°C/s [8],[15].The measurement of blood temperature during laser based treatment of tissues [19] and intravascular interventional surgery [20] also records steep spatial temperature gradients.

Chirped FBG (CFBG), particularly having a linear chirp profile, have been used to extend the functionality of uniform FBGs in this application [21]. While prior to the early 2010s CFBGs have been mainly used as mechanical strain sensors [22],[23], recent works have shown the possibility of using CFBGs for biomedical applications in thermal ablation [24]. The principle of operation is encoded in the CFBG spectrum: a different CFBG reflection spectrum is observed as a function of each temperature spatial distribution. In particular, Korganbayev *et al.* [15] in 2018 proposed a method for demodulating the CFBG by means of an iterative optimization technique, that estimates the temperature profile by applying the same thermal profile to a CFBG theoretical model [3] and observing when the estimated and measured spectra show the best agreement.

A drawback of this arrangement is that the temperature sensitivity of a standard CFBG on a glass fiber is typically 10 pm/°C, which results in small spectral variations in the inner CFBG bandwidth. In order to increase the sensitivity, recent works showed promising results on the fabrication of CFBGs on polymethyl methacrylate (PMMA) polymer optical fiber (POF) [25],[26],[27]. Marques *et al.* [26] reported the inscription of a CFBG on an undoped step-index POF with sensitivity of -131 pm/°C. Min *et al.* [27] reported a tunable CFBG on a microstructed POF (mPOF) tapered fiber with benzyl dimethyl ketal (BDK) doping achieving -56.7 pm/°C sensitivity. Thus, by utilizing a CFBG on a single-mode POF in lieu of a standard glass fiber results in a thermal sensitivity increase of about one order of magnitude, which allows spectral detection technique to be more effective, and allow the measurement of temperature patterns with a better accuracy.

In this work we describe the fabrication and application of an mPOF CFBG for the detection of temperature patterns in thermal ablation. A mPOF CFBG with sensitivity -191.4 pm/°C and 1 cm length has been fabricated and used for *in situ* detection of temperature pattern in a radiofrequency ablation setup [28]. In a first experiment, the mPOF CFBG has been located on a heating plate, detecting a linear temperature profile. Then, the mPOF CFBG has been used for detecting the temperature in proximity of the ablation thermal peak, with a profile close to Gaussian. A demodulation technique for the mPOF CFBG is introduced, which allows converting the CFBG spectrum into the temperature measured in each section of the grating, with 1 mm spatial resolution. The proposed result represent an important benchmark for application of PMMA CFBG in healthcare for detection of thermal maps with narrow spatial resolution, with immediate application in thermo-therapies.

II. mPOF CFBG Inscription and Interrogation

A. Inscription

The mPOF used in this work was a three ring microstructure PMMA POF with BDK doped in the core [29]. Due to the average hole diameter and pitch in the fiber, we believe the mPOF shows an endlessly single mode behavior [29]. Before the use, about 20 cm length piece was pre-annealed at 70°C for 24 hours in order to remove residual stress during the drawing process. Then, the fiber sample was connected to the ferrule on one end, in order to connect it to a standard single mode fiber (SMF) through a mating sleeve: due to the different diameter between the mPOF and the SMF, it was necessary to partially etch the end-side of the mPOF fiber to match the size of the SMF. For the non-uniform etching process, the polymer fiber was tilted and immersed in a container full of 2:1 mixed acetone and liquid alcohol; one linear translation stage was programmed to move the fiber with constant speed performing a non-uniform etching, with a process similar to [30]. Afterwards, glue was used to fix the mPOF-SMF connector, drying the glue at room temperature for several hours to stabilize the structure [30]. Finally, the end face of the mPOF fiber was polished with sand paper to enhance the end face quality.

A 248 nm wavelength pulsed Coherent Krypton Fluoride (KrF) excimer laser system was employed for the chirped Bragg grating inscription with a 2.5 mJ pulse [27] (see Fig.1). The laser beam profile was measured as a rectangular Tophat function of 6.0×1.5 mm^2 size and divergence 2×1 mrad^2, the UV beam focused on the fiber utilizing a plano-convex cylindrical lens with an effective focal length of 200.0 mm.

The grating inscription was performed using 1067.03 nm phase mask, under 1% strain, in order to obtain a chirp profile [31]. The result is a 10 mm grating corresponding to the physical length of the phase mask, whereas the chirp profile is obtained through the strain pattern .

Fig. 2 shows the obtained CFBG and non-uniform tapering on mPOF, as measured on the experimental setup. The grating length of 10 mm results in a maximum reflectivity of -34.27 dB measured by spectral analysis, and having about 25 dB amplitude over the noise floor. The full-width half-maximum (FWHM) bandwidth is 0.94 nm, which corresponds to a chirp rate approximately 0.09 nm/mm.
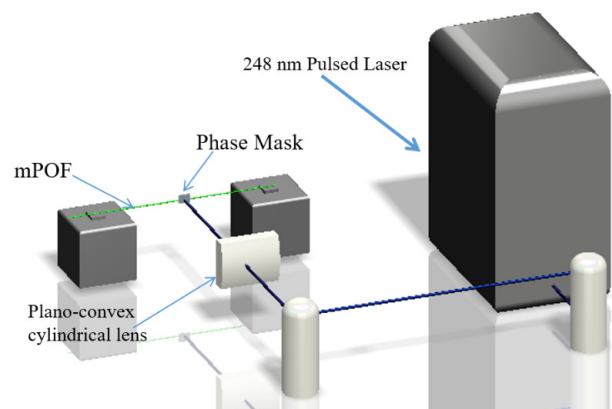

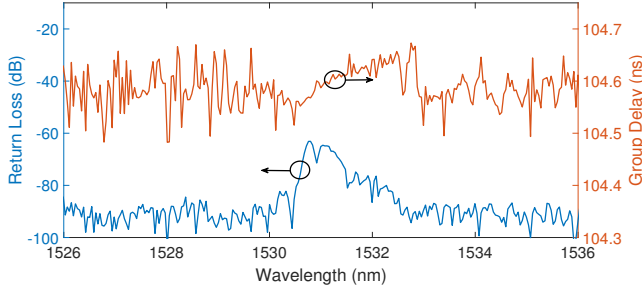Fig. 1. Schematic of CFBG inscription on mPOF.

Fig. 2. Reflection spectrum (left) and group delay (right) of mPOF CFBG in reference condition, before exposure to thermal ablation.
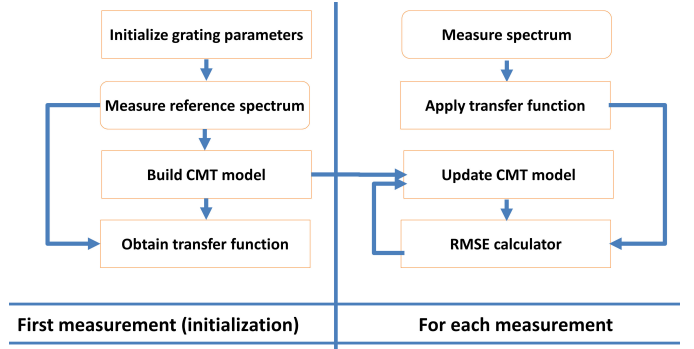
Fig. 3. Reconstruction algorithm. Before the first measurement we input model grating parameters. After, transfer function, ratio of measured reference spectrum and CMT model spectrum without applied temperature, is calculated. Then, algorithm calculates root-mean-square error (RMSE) between filtered measured spectrum and updated CMT model to minimize cost function. As a result, the final temperature profile is obtained.

B. Experimental Setup

The experimental setup used for the CFBG analysis has been arranged in order to expose the grating to spatially uniform and non-uniform thermal gradients, in order to observe the variations of the spectrum under different conditions. This task has been implemented using a water bath in order to obtain a uniform temperature, and a hot plate in order to induce a thermal gradient. Finally, the CFBG has been exposed to a thermal ablation using a radiofrequency generator based setup.

For the experimental analysis, we used a Luna OBR4600 optical backscatter reflectometer (OBR, Luna Inc., Roanoke, VA, US) as an interrogation setup to detect the mPOF CFBG spectrum with 1525-1610 nm wavelength range and 33 pm wavelength resolution. The use of an OBR instead of a standard interrogator of FBG analyzer allows the detection of a smaller amount of power, since the PMMA fiber and its connector are lossy devices. In addition, the OBR can measure the group delay.

The experimental setup for calibration and linear temperature profile consists of a water bath, hot plate (IKA magnetic stirrer/C-Mag HS4) and reference thermometer (IKA electronic contact thermometer/ETS D-5, accuracy $\pm 0.2°C$). For temperature measurement with mPOF CFBG during radiofrequency ablation experiment, a Leanfa Hybrid generator (450 kHz) was used to ablate porcine liver phantom [24].

C. Temperature detection

In order to detect the temperature profiles in each experimental validation, the method of spectral reconstruction developed in [15] and also reported in [8] has been adjusted to the specific type of grating, and implemented. A schematic of the algorithm is shown in Fig.3.

In this method, we assume that the temperature profile over the grating length has a known shape, dependent on a small set of parameters. Thus, a model of the grating built by coupled mode theory (CMT) [3] has been implemented, estimating the grating parameters [15]. Subsequently, at each measurement, a temperature profile is applied to the CMT model until the root mean square error between the simulated grating and the measured spectrum is minimized. This method has been consolidated in [15], and allows the detection of either a linear thermal pattern, such as the gradient observed by exposing the CFBG to a hot-plate setup, or a Gaussian-shaped pattern as

typically observed during radiofrequency [24] or laser [15] ablation, which is the main application area for the mPOF CFBG. Calling $\Delta T(z)$ the temperature profile, where z is the axis of the fiber, a linear profile is expressed as a 2-parameters estimation:

$$\Delta T(z) = A_0 + A_1 \cdot z \tag{1}$$

where A_1 is the thermal gradient, and A_0 is the temperature offset. For a thermal ablation pattern [15], we assume a Gaussian pattern:

$$\Delta T(z) = A \cdot exp\left[-\frac{(z - z_0)^2}{2\sigma^2} \right] \tag{2}$$

where A, z_0, and σ are the amplitude, center value, and standard deviation respectively.

It should be highlighted that high temperature sensitivity of mPOF compared with silica CFBG (about 15 times larger in magnitude) can provide unprecedented temperature profile measurement sensitivity [26]: since a local temperature variation causes a much larger shift of the respective portion of the grating, compared to [15] we observe a much larger spectral variation that is helpful to the spectral reconstruction method.

The hereby proposed temperature reconstruction technique maintains the same procedural steps reported in [15].While in [15] the grating under analysis was a silica CFBG having a much larger chirp coefficient, in the present work it is necessary to adjust the model to match the geometrical and optical parameters of the mPOF grating taking into account, in particular, the significant changes in terms of chirp rate coefficient (~1 order of magnitude narrower than a silica fiber) and thermal sensitivity (~1 order of magnitude larger and with opposite sign than a silica fiber). The solution that we propose is to maintain a relatively high number of simulated gratings (M=100), which provides an adequate discretization profile of each element constituting the chirped grating, and to estimate the other parameters from the optical spectrum: 1529.5-1530.7 wavelength bandwidth, grating strength kL_g=0.34, refractive index change δn_{eff}=10^{-5}, refractive index of mPOF $n_{eff} =$

1.4895, and thermal sensitivity -191.4 pm/°C. The main variation that we need to implement is in the grating length, as we artificially set the length of the overall CFBG to 10 cm, rather than 1 cm as its geometrical size. The reason for this change is that the temperature reconstruction method is effective in converting the spectral changes when each discrete grating element is spaced from the adjacent elements; this condition occurs for gratings having chirp rate of 1 nm/mm to 2 nm/mm as it was applied in [15] but does not apply to the present mPOF CFBG that has a chirp rate of 0.09 nm/mm, much lower than previous gratings. Thus, in order to maintain the structure of the algorithm without changing the optimization routine, we artificially expand the grating length by a factor 10 in order to have an artificial chirp rate of 0.94 nm/mm, similar to the previous values reported in [15], and compensating in part the limitations of the inscription setup to fabricate wideband CFBGs on a fiber with polymer compound. After inputting all the parameters of the grating including the artificial length, the algorithm computes the optimization routine and extract the temperature profile over the grating artificial length, that is then rescaled down by a factor 10 to the 0-1 cm axis.

III. EXPERIMENTS

A. Calibration

Before calibration the mPOF CFBG has been placed inside the water bath for 12 hours in order to absorb all possible water and, subsequently, prevent humidity effect on spectral shift during the experiment. Calibration of the CFBG has been done through the measurements of a spatially uniform temperature: the CFBG is positioned inside the water bath and the reference temperature is measured with the thermometer. The temperature has been increased from 24.5°C to 37.0°C, measuring the CFBG spectrum during the heating cycle; this range allows the full CFBG spectrum to be within the wavelength range of the interrogator, and is compatible with biomedical applications [20],[8]. For each measurement the Bragg wavelength has been estimated by calculating the center of the FWHM of the grating. In Fig. 4, the spectra of the FBG during thermal calibration are observed: it is possible to notice, as expected by [26], that the spectrum shifts towards the shortest wavelengths during the heating cycle. As shown in Fig. 5, by evaluating the Bragg wavelength shift as a function of temperature, the thermal sensitivity of the CFBG sensor has been estimated as -191.4 pm/°C, after fitting to a linear model. This value is similar to sensitivity achieved in [32] equal to -180.0 pm/°C. This obtained sensitivity value has been used in the following experiments, in the CMT model for spectral reconstruction. The small errors in calibration can be explained by not uniform heat distribution in the water bath, heat absorption effect, accuracy of the thermometer, and to a non-linear thermal coefficient of the PMMA fiber [33]. The sensitivity observed for this grating is similar to previously reported POF gratings operating in near-infrared [26],[27] and much larger than cyclo-olefin copolymer [34] that has lesser sensitivity to humidity.
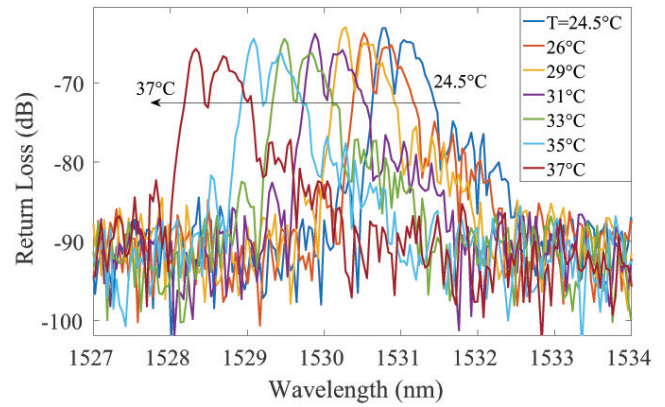

Fig. 4. Reflection spectra of the mPOF CFBG, positioned in water bath during temperature increase, for different temperatures.
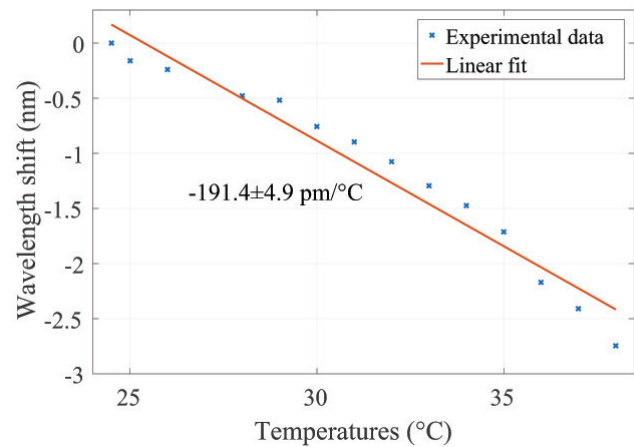

Fig. 5. mPOF CFBG central wavelength shift as a function of temperature; the chart shows the experimental data and a linear fit.

B. Linear gradient

Following the method in [15] and used also in [35] to calibrate a CFBG by means of a controlled heating source, an experiment has been designed having a linear thermal gradient in order to evaluate the capability of the CFBG to respond to a non-uniform spatial gradient [36].

For linear temperature gradient, the tip of the CFBG sensor corresponding to the right portion (longest wavelengths) of the spectrum has been placed at the center of the hot plate, while the tail (shortest wavelengths) has been positioned at 2 cm from the plate. Due to the fact that temperature acting on the tip is higher than a tail temperature, we can observe an approximately linear thermal gradient along the CFBG length. The gradient is induced between the tip and the tail of the grating by the different amount of heating acting on each side of the CFBG: considering the short length of the CFBG, we assume that the temperature profile follows the linear pattern as in Eq.(1).

The Fig. 7 shows that in this setup, as expected, the thermal reconstruction returns a linear gradient along the grating. The thermal map reports that as the plate heats, and temperature increases from the tip to the tail of the grating, the gradient
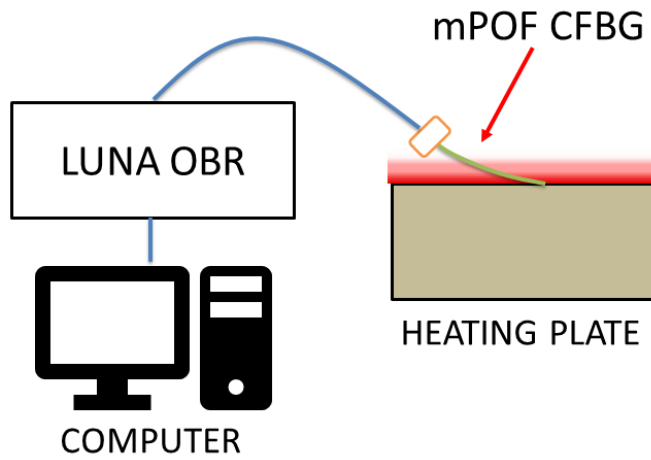
Fig. 6. Schematic of linear gradient experiment: tail of the CFBG is placed at distance from heating plate and tip is fixed on the plate. LUNA OBR measures mPOF CFBG spectra during the heating experiment.
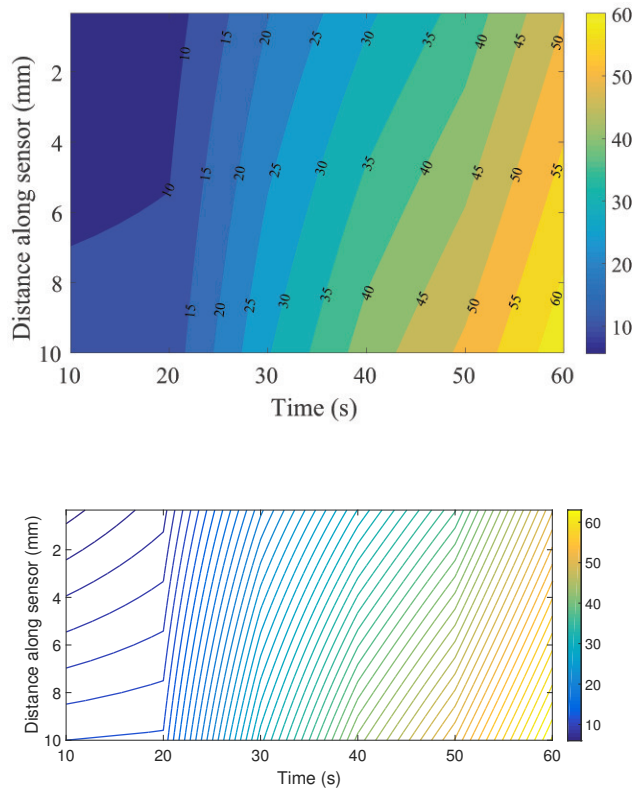

Fig. 7. Measurement of linear temperature gradient with a mPOF CFBG as a function of distance along grating and time. The colorbar shows temperature in °C degrees. Upper chart: thermal map; Lower chart: isothermal curves.

progressively enlarges until the hot plate reaches 60°C; at this time, the tail of the grating is exposed to 49°C, accounting for a gradient of 11°C/cm. This experiments shows that the CFBG responds in a different way to a non-uniform pattern, and the spectral reconstruction method can estimate the thermal map.

C. Thermal ablation

This experiment focused on temperature measurement with mPOF CFBG during radiofrequency ablation (RFA) on porcine liver. RFA is a medical treatment aimed at the minimally invasive ablation of tumors after their localization, and has been practiced as a clinical procedure [28], [37]. The use of fiber optic sensors in measurement of the thermal patterns during RFA was introduced in [24]: in this work, the use of the mPOF CFBG provides a much larger sensitivity to temperature variation (18.7 times larger than [24]).

The mPOF CFBG has been placed in proximity of a radiofrequency applicator (Fig. 8) to measure temperature at the edge of ablated volume. The applicator is a research-grade single-tip electrode having 5 mm thickness and percutaneously shaped tip, inserted *in situ* at the center of the target zone. The applicator is connected to the RF generator, that supplied a 450 kHz continuous power (50 W) to the electrode. The power has been maintained constant through the experiment for 27 seconds, to mimic a rapid thermal ablation of a small target zone. The applicator has been placed at a distance of approximately 10 mm from the CFBG sensor, in order to avoid exposing the grating to excessive temperature. The reflection spectrum of the mPOF CFBG has been progressively detected by LUNA OBR4600 and further analyzed using the spectral reconstruction technique; for the temperature gradient estimation, we use the Gaussian model in Eq. (2).
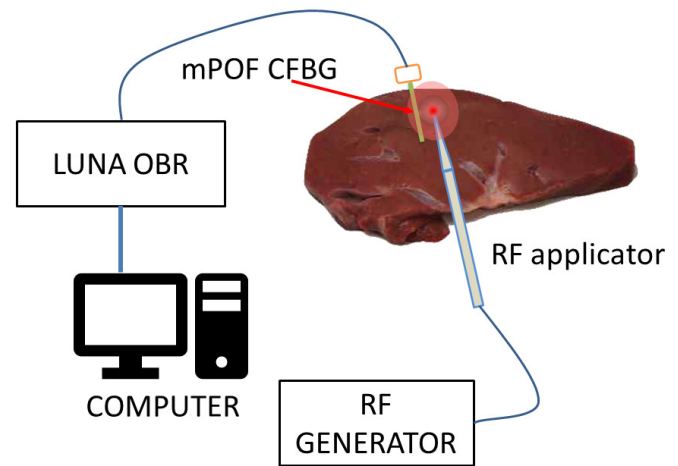

Fig. 8. Schematic of thermal ablation experiment: the LUNA OBR measures spectra from mPOF CFBG, which is placed in proximity of RF applicator during the ablation.

The results of thermal reconstruction are shown in Figs. 9 and 10. Fig. 9 shows the whole thermal map; it is clearly seen in Fig. 10 that temperature reaches maximum 8°C at 9 s and starts decreasing after after 18 s, that correlates with the ablation cycle during experiment. Results are in line with [24] considering the temperature regions outside of the central peak value. The RF power has been automatically disconnected by the RF generator after 18 s, in correspondence to the impedance of the tissue rising over threshold value [24]: this causes the tissue to cool down until reaching room temperature.
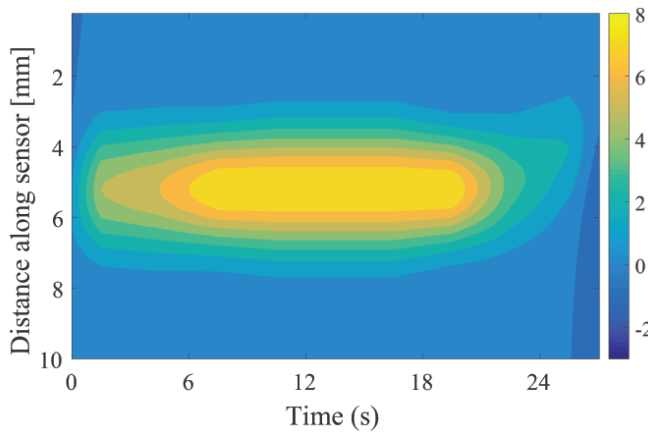
Fig. 9. Measurement of Gaussian temperature gradient with a mPOF CFBG: thermal profile reconstructed with the CFBG as a function of distance along grating and time during ablation. The colorbar shows temperature in °C degrees.
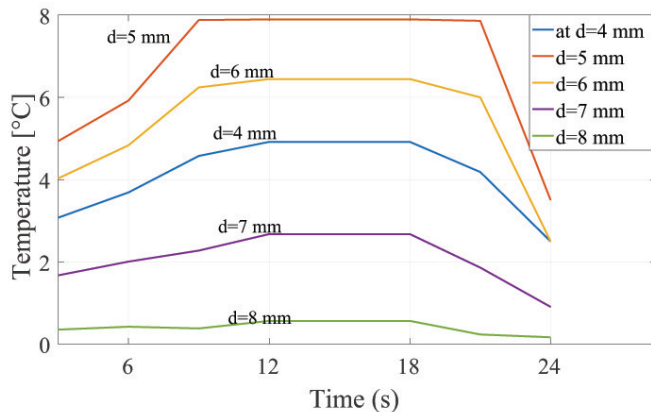

Fig. 10. Temperature graphs for Gaussian-shaped RFA temperature profile; the chart reports the temperature as a function of time, for different values of position along the grating length d.

IV. CONCLUSION

In this work, we reported the measurement of thermal profiles using a mPOF CFBG fiber optic sensor, with a detection method based on spectral reconstruction. The higher sensitivity to temperature variations (-191.4 pm/°C) with respect to glass fiber, and the low chirp rate of the mPOF grating require modification of the reconstruction algorithm. We have conducted two sets of experiments: linear temperature profile along 10 mm mPOF CFBG, and a radiofrequency ablation that induces Gaussian-shaped temperature gradient. Experiments validate that proposed use of mPOF CFBG can provide significant advantages for thermal sensing in biomedical applications. Future work will be addressed to evaluate the response of the mPOF CFBG in closer proximity to the applicator, using a longer grating length and possibly a larger chirp rate, and to improve the spectral reconstruction method to work with specific mPOF CFBG coefficients.

REFERENCES

[1] S. J. Mihailov, "Fiber bragg grating sensors for harsh environments," *Sensors*, vol. 12, no. 2, pp. 1898–1918, 2012.

[2] A. D. Kersey, M. A. Davis, H. J. Patrick, M. LeBlanc, K. Koo, C. Askins, M. Putnam, and E. J. Friebele, "Fiber grating sensors," *Journal of lightwave technology*, vol. 15, no. 8, pp. 1442–1463, 1997.

[3] T. Erdogan, "Fiber grating spectra," *Journal of lightwave technology*, vol. 15, no. 8, pp. 1277–1294, 1997.

[4] A. Othonos and K. Kalli, *Fiber Bragg gratings: fundamentals and applications in telecommunications and sensing.* Artech House, 1999.

[5] Y. Wang, J. Gong, D. Y. Wang, B. Dong, W. Bi, and A. Wang, "A quasi-distributed sensing network with time-division-multiplexed fiber bragg gratings," *IEEE Photonics Technology Letters*, vol. 23, no. 2, pp. 70–72, 2011.

[6] S. W. Tyler, J. S. Selker, M. B. Hausner, C. E. Hatch, T. Torgersen, C. E. Thodal, and S. G. Schladow, "Environmental temperature sensing using raman spectra dts fiber-optic methods," *Water Resources Research*, vol. 45, no. 4, 2009.

[7] E. Schena, D. Tosi, P. Saccomandi, E. Lewis, and T. Kim, "Fiber optic sensors for temperature monitoring during thermal treatments: an overview," *Sensors*, vol. 16, no. 7, p. 1144, 2016.

[8] D. Tosi, E. Schena, C. Molardi, and S. Korganbayev, "Fiber optic sensors for sub-centimeter spatially resolved measurements: Review and biomedical applications," *Optical Fiber Technology*, vol. 43, pp. 6–19, 2018.

[9] D. J. Webb, M. Hathaway, D. A. Jackson, S. Jones, L. Zhang, and I. Bennion, "First in-vivo trials of a fiber bragg grating based temperature profiling system," *Journal of biomedical optics*, vol. 5, no. 1, pp. 45–51, 2000.

[10] M. W. Rothhardt, "Fabrication and applications of draw tower gratings," in *Bragg Gratings, Photosensitivity, and Poling in Glass Waveguides.* Optical Society of America, 2016, pp. BTh1B–1.

[11] B. J. Soller, D. K. Gifford, M. S. Wolfe, and M. E. Froggatt, "High resolution optical frequency domain reflectometry for characterization of components and assemblies," *Optics Express*, vol. 13, no. 2, pp. 666–674, 2005.

[12] M. Froggatt and J. Moore, "High-spatial-resolution distributed strain measurement in optical fiber with rayleigh scatter," *Applied Optics*, vol. 37, no. 10, pp. 1735–1740, 1998.

[13] Z. Ding, C. Wang, K. Liu, J. Jiang, D. Yang, G. Pan, Z. Pu, and T. Liu, "Distributed optical fiber sensors based on optical frequency domain reflectometry: A review," *Sensors*, vol. 18, no. 4, p. 1072, 2018.

[14] J. Hervás, D. Barrera, J. Madrigal, and S. Sales, "Microwave photonics filtering interrogation technique under coherent regime for hot spot detection on a weak fbgs array," *Journal of Lightwave Technology*, vol. 36, no. 4, pp. 1039–1045, 2018.

[15] S. Korganbayev, Y. Orazayev, S. Sovetov, A. Bazyl, E. Schena, C. Massaroni, R. Gassino, A. Vallan, G. Perrone, P. Saccomandi *et al.*, "Detection of thermal gradients through fiber-optic chirped fiber bragg grating (cfbg): Medical thermal ablation scenario," *Optical Fiber Technology*, vol. 41, pp. 48–55, 2018.

[16] R. C. Martin, C. R. Scoggins, and K. M. McMasters, "Safety and efficacy of microwave ablation of hepatic tumors: a prospective review of a 5-year experience," *Annals of surgical oncology*, vol. 17, no. 1, pp. 171–178, 2010.

[17] P. L. Pereira, "Actual role of radiofrequency ablation of liver metastases," *European radiology*, vol. 17, no. 8, pp. 2062–2070, 2007.

[18] P. Saccomandi, E. Schena, M. A. Caponero, F. M. Di Matteo, M. Martino, M. Pandolfi, and S. Silvestri, "Theoretical analysis and experimental evaluation of laser-induced interstitial thermotherapy in ex vivo porcine pancreas," *IEEE Transactions on Biomedical Engineering*, vol. 59, no. 10, pp. 2958–2964, 2012.

[19] W. Liu, Y. Kong, X. Shi, X. Dong, H. Wang, J. Zhao, and Y. Li, "Determination of temperature and residual laser energy on film fiber-optic thermal converter for diode laser surgery," *Computer Assisted Surgery*, vol. 22, no. sup1, pp. 251–257, 2017.

[20] X. Zou, N. Wu, Y. Tian, J. Ouyang, K. Barringhaus, and X. Wang, "Miniature fabry–perot fiber optic sensor for intravascular blood temperature measurements," *IEEE Sensors Journal*, vol. 13, no. 6, pp. 2155–2160, 2013.

[21] P. C. Won, J. Leng, Y. Lai, and J. A. Williams, "Distributed temperature sensing using a chirped fibre bragg grating," *Measurement Science and Technology*, vol. 15, no. 8, p. 1501, 2004.

[22] M. Pisco, A. Iadicicco, S. Campopiano, A. Cutolo, and A. Cusano, "Structured chirped fiber bragg gratings," *Journal of Lightwave Technology*, vol. 26, no. 12, pp. 1613–1625, 2008.

[23] S. Yashiro, T. Okabe, N. Toyama, and N. Takeda, "Monitoring damage in holed cfrp laminates using embedded chirped fbg sensors," *International Journal of Solids and Structures*, vol. 44, no. 2, pp. 603–613, 2007.

[24] D. Tosi, E. G. Macchi, M. Gallati, G. Braschi, A. Cigada, S. Rossi, G. Leen, and E. Lewis, "Fiber-optic chirped fbg for distributed thermal monitoring of ex-vivo radiofrequency ablation of liver," *Biomedical optics express*, vol. 5, no. 6, pp. 1799–1811, 2014.

[25] D. J. Webb, "Fibre bragg grating sensors in polymer optical fibres," *Measurement Science and Technology*, vol. 26, no. 9, p. 092004, 2015.

[26] C. Marques, P. Antunes, P. Mergo, D. Webb, and P. André, "Chirped bragg gratings in pmma step-index polymer optical fiber," *IEEE Photonics Technology Letters*, vol. 29, no. 6, pp. 500–503, 2017.

[27] R. Min, B. Ortega, and C. Marques, "Fabrication of tunable chirped mpof bragg gratings using a uniform phase mask," *Optics express*, vol. 26, no. 4, pp. 4411–4420, 2018.

[28] S. Rossi, M. Di Stasi, E. Buscarini, P. Quaretti, F. Garbagnati, L. Squassante, C. Paties, D. Silverman, and L. Buscarini, "Percutaneous rf interstitial thermal ablation in the treatment of hepatic cancer." *AJR. American journal of roentgenology*, vol. 167, no. 3, pp. 759–768, 1996.

[29] X. Hu, G. Woyessa, D. Kinet, J. Janting, K. Nielsen, O. Bang, and C. Caucheteur, "Bdk-doped core microstructured pmma optical fiber for effective bragg grating photo-inscription," *Optics letters*, vol. 42, no. 11, pp. 2209–2212, 2017.

[30] D. Sáez-Rodríguez, R. Min, B. Ortega, K. Nielsen, and D. J. Webb, "Passive and portable polymer optical fiber cleaver," *IEEE Photonics Technology Letters*, vol. 28, no. 24, pp. 2834–2837, 2016.

[31] L. Dong, J. Cruz, L. Reekie, and J. Tucknott, "Fabrication of chirped fibre gratings using etched tapers," *Electronics Letters*, vol. 31, no. 11, pp. 908–909, 1995.

[32] H. Liu, H. Liu, G. Peng, and T. W. Whitbread, "Tunable dispersion using linearly chirped polymer optical fiber bragg gratings with fixed center wavelength," *IEEE photonics technology letters*, vol. 17, no. 2, pp. 411–413, 2005.

[33] A. Sophie, M. Patrick, O. Heidi, G. Thomas, T. Hugo, C. A. Marques, D. J. Webb, G.-D. Peng, P. Mergo, and B. Francis, "Thermal effects on the photoelastic coefficient of polymer optical fibers," *Optics letters*, vol. 41, no. 11, pp. 2517–2520, 2016.

[34] M. Rosenberger, G. Roth, B. Adelmann, B. Schmauss, and R. Hellmann, "Temperature referenced planar bragg grating strain sensor in fs-laser cut coc specimen," *IEEE Photonics Technology Letters*, vol. 29, no. 11, pp. 885–888, 2017.

[35] P. Saccomandi, A. Varalda, R. Gassino, D. Tosi, C. Massaroni, M. A. Caponero, R. Pop, S. Korganbayev, G. Perrone, M. Diana *et al.*, "Linearly chirped fiber bragg grating response to thermal gradient: from bench tests to the real-time assessment during in vivo laser ablations of biological tissue," *Journal of biomedical optics*, vol. 22, no. 9, p. 097002, 2017.

[36] P. Bettini, E. Guerreschi, and G. Sala, "Development and experimental validation of a numerical tool for structural health and usage monitoring systems based on chirped grating sensors," *Sensors*, vol. 15, no. 1, pp. 1321–1341, 2015.

[37] T. Livraghi, L. Solbiati, M. F. Meloni, G. S. Gazelle, E. F. Halpern, and S. N. Goldberg, "Treatment of focal liver tumors with percutaneous radio-frequency ablation: complications encountered in a multicenter study," *Radiology*, vol. 226, no. 2, pp. 441–451, 2003.